

Nonlinear Passive Stiffness using Mechanical Singularity and Its Application for Four-legged Robot

Masafumi OKADA [†] and Shintaro KINO [‡]

[†] Dept. of Mechanical Sciences and Engineering, Tokyo TECH

[‡] Dept. of Mechanical and Intelligent Systems Engineering, Tokyo TECH

Abstract To introduce a passive compliant mechanism for robot joints is an effective way for impact absorption. However, because robot joints also require high torque transmission characteristic, the simultaneous implementation of stiffness and softness is a significant issue. In this paper, we develop a torque transmission mechanism with nonlinear passive stiffness that realizes from zero to extremely high stiffness using mechanical singularity. The analysis of nonlinearity of the stiffness is established and the experimental evaluations are shown. A four-legged robot with the proposed mechanism is designed and the effectiveness of high nonlinearity of the proposed mechanism is shown by landing and walking simulation.

1 Introduction

In the robot control, the impact force damages to the robot body and its environments, this causes a breakage of members, failure of control system and hurt of people. From flexibility and safety points of view, to introduce softness to robot members or joints gives an effective solution.

For the realization of a soft robot, (1) active compliance (Paul and Shimano, 1976; Hanafusa and Asada, 1978; Hogan, 1980; Salisbury, 1980; Hogan), (2) passive compliance, and (3) programmable passive compliance (L-Kovitz et al., 1991; Morita et al., 1999; Okada et al., 2001; Yamaguchi et al., 1998) are proposed so far. The active compliance does not completely realize softness in high frequency (for impact force) because of the low frequency response of actuators and/or sensors. The programmable passive compliance requires the additional actuator and it increases the weight and volume of the robot. On the other hand, passive compliance is simple and effective for softness of the robots. Because robots also require high torque transmission for task executions, the simultaneous realization of stiffness and softness is an important issue, and highly nonlinear stiffness will give us an effective solution. In this paper, we develop a nonlinear passive stiffness mechanism by using the nonlinearity of mechanism. This mechanism realizes (a) zero-stiffness using mechanical singularity and (2) high nonlinearity of passive stiffness. A four-legged robot with the proposed mechanism is designed and the effectiveness of high nonlinearity of the proposed mechanism is shown by walking simulation.

2 Zero-stiffness using mechanical singularity

2.1 Mechanism

Joints and links configuration of the proposed mechanism is shown in figure 1-(a). The rotational axes of joints $R_1 \sim R_5$ are set along with z , x , x , z and z -axis respectively. Their

rotation angles are defined by $\theta_1 \sim \theta_4$ and ϕ . Figure 1-(b) shows the cross-section drawing of the prototype. The input torque τ_{in} that works Disk D_{in} is transmitted to τ_{out} on Disk D_{out} through Link L . Roller bearings are used for R_2 and R_3 , ball bearings are used for other joints. To reduce the influence of backlash, pre-tension is added to link L by tightening the screw in S .

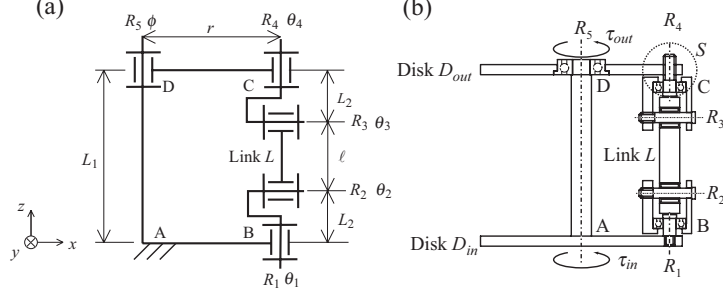


Figure 1. Joints and links configuration and cross-section view of the proposed mechanism

2.2 Zero-stiffness analysis based on null space of Jacobian matrix of constraints

In generally, the degree-of-freedom (DOF) F of a 3D mechanism is calculated by $F = 6(n - 1) - \sum_i (6 - i)n_i$, where n means the number of links and n_i means the summation of the number of i -DOF revolute pairs. The DOF of the proposed mechanism F_p is calculated by $F_p = 6(5 - 1) - (6 - 1)5 = -1$. Because $\ell = L_1 - 2L_2$ yields the dependency of the constraints, we obtain $F_p = 0$, which means this mechanism does not move from mechanical DOF point of view. On the other hand, consider the constraints of this mechanism. By considering the closed loop of $A \rightarrow B \rightarrow C \rightarrow D \rightarrow A$, there are six independent constraints for position and orientation as follows.

$$f(\theta_1, \theta_2, \theta_3, \theta_4, \phi) = 0 \quad (2.1)$$

$$g(\theta_1, \theta_2, \theta_3, \theta_4, \phi) = I_3 \quad (2.2)$$

where I_3 means 3×3 identity matrix. Because it is clear that $g \in R^{3 \times 3}$ is an orthogonal matrix, equation (2.2) is equivalent to the condition so that the diagonal elements of g are equal to 1. These constraints are satisfied when $\theta_i = 0$, $\phi = 0$. Consider the minimal change $\Delta\theta_i$ and $\Delta\phi$. By neglecting more than second order minimal value, f and g are approximated as follows.

$$\begin{bmatrix} f(\Theta + \Delta\Theta) \\ g(\Theta + \Delta\Theta) \end{bmatrix} = \begin{bmatrix} f(\Theta) \\ g(\Theta) \end{bmatrix} + J(\Theta)\Delta\Theta \quad (2.3)$$

$$\Theta = [\theta_1 \quad \theta_2 \quad \theta_3 \quad \theta_4 \quad \phi]^T \quad (2.4)$$

$$\Delta\Theta = [\Delta\theta_1 \quad \Delta\theta_2 \quad \Delta\theta_3 \quad \Delta\theta_4 \quad \Delta\phi]^T \quad (2.5)$$

$$J(\Theta) = \begin{bmatrix} \frac{\partial f}{\partial \theta_1} & \frac{\partial f}{\partial \theta_2} & \frac{\partial f}{\partial \theta_3} & \frac{\partial f}{\partial \theta_4} & \frac{\partial f}{\partial \phi} \\ \frac{\partial g}{\partial \theta_1} & \frac{\partial g}{\partial \theta_2} & \frac{\partial g}{\partial \theta_3} & \frac{\partial g}{\partial \theta_4} & \frac{\partial g}{\partial \phi} \end{bmatrix} \quad (2.6)$$

When the second term of the right-hand side in equation (2.3) is equal zero, $\Theta + \Delta\Theta$ also satisfies the constraints (2.1) and (2.2), which means this mechanism can move to the direction of $\Delta\Theta$

without any strain of members, that is to say stiffness of this mechanism is equivalent to zero to the direction of $\Delta\Theta$. When the rank of $J \in R^{6 \times 5}$ is less than 5, non-zero $\Delta\Theta$ exists, which comes from the mechanical singularity. On the proposed mechanism, rank of J at $\Theta = 0$ is calculated as rank $J = 3 (< 5)$ and the orthogonal bases of the null-space of J are obtained as

$$\Delta\Theta_1 = \begin{bmatrix} -0.71 & 0 & 0 & 0.71 & 0 \end{bmatrix}^T \quad (2.7)$$

$$\Delta\Theta_2 = \begin{bmatrix} 0.33 & -0.41 & 0.41 & 0.33 & -0.66 \end{bmatrix}^T \quad (2.8)$$

Equation (2.7) means link L rotates around z axis. On the other hand, equation (2.8) means the upper disk can rotate $\Delta\phi$ as shown in figure 2, which means this mechanism has zero-stiffness on R_5 axis when $\Theta = 0$.

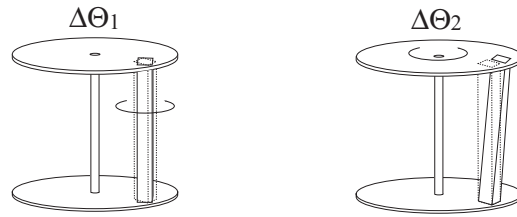


Figure 2. Rotation of mechanism on behalf of $\Delta\Theta_i$

3 Stiffness analysis of the mechanism

3.1 Prototype of the proposed mechanism

The rotation of D_{out} by ϕ yields nonlinear spring characteristic because of the elasticity of link L . Figure 3 shows the prototype of the proposed mechanism and the twist motion of the mechanism. In this section, only link L is assumed to be elastic.

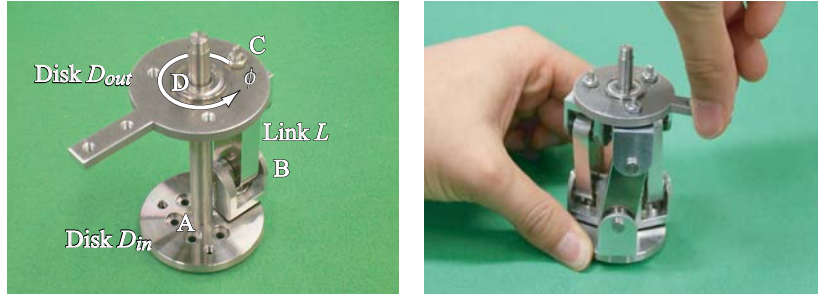


Figure 3. Prototype of the proposed mechanism and its twist motion

3.2 Force and momentum working on L

In this section, we consider the force and momentum that works to L . Assume that the length of link L changes from ℓ to $\ell + \lambda$ due to the rotation by ϕ on R_5 axis as shown in figure 4. Figure

4-(b) shows the top view of figure 4-(a). One straight line passing through points B and C is

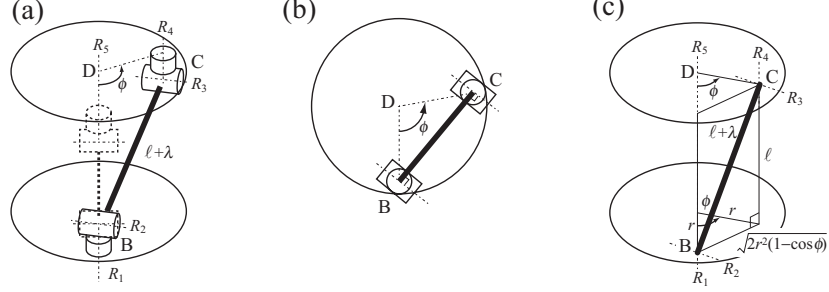


Figure 4. Relationship between ϕ and $\ell + \lambda$

uniquely decided and R_1, R_4 rotate so that R_2, R_3 axes are orthogonal to this line. The rotation angles are represented by $-\theta_1 = \theta_4 = (\pi - \phi)/2$. This result is derived from two parallelisms of R_1, R_4 axes and R_2, R_3 axes. From these considerations, any momentum do not work but only tension for the length direction works to link L with respect to the rotation by ϕ .

3.3 Calculation of stiffness

We calculate torsional stiffness K_ϕ on R_5 axis of this mechanism. K_ϕ is defined by

$$K_\phi(\phi) = \frac{d\tau(\phi)}{d\phi} \quad (3.1)$$

where τ means the restorative force. This definition means the stiffness at ϕ in proximity.

The spring constant of link L for length direction is defined by K_L (assuming to be a linear spring). Assume that torsional torque τ on R_5 axis yields rotation by ϕ and the length of link L is changed from ℓ to $\ell + \lambda$. The accumulated kinetic energy E is represented by

$$E = \int_0^\phi \tau(\phi) d\phi = \int_0^\lambda K_L \lambda d\lambda = \frac{1}{2} K_L \lambda^2 \quad (3.2)$$

The differential of E with respect to ϕ gives torque τ as follows.

$$\frac{dE}{d\phi} = \tau(\phi) = K_L \lambda \frac{d\lambda}{d\phi} \quad (3.3)$$

The geometry shown in figure 4-(c) gives

$$2r^2(1 - \cos \phi) + \ell^2 = (\ell + \lambda)^2 \quad (3.4)$$

by cosine formula and Pythagorean theorem, and λ is represented by

$$\lambda = \sqrt{2r^2(1 - \cos \phi) + \ell^2} - \ell \quad (3.5)$$

The differential of λ with respect to ϕ gives

$$\frac{d\lambda}{d\phi} = \frac{r^2 \sin \phi}{\sqrt{2r^2(1 - \cos \phi) + \ell^2}} \quad (3.6)$$

Equations (3.3), (3.5) and (3.6) lead torque τ by the function of ϕ as follows.

$$\tau(\phi) = K_L \left(r^2 \sin \phi - \frac{\ell r^2 \sin \phi}{L_\phi(\phi)} \right), \quad L_\phi(\phi) = \sqrt{2r^2(1 - \cos \phi) + \ell^2} \quad (3.7)$$

Stiffness K_ϕ is obtained from the differential of equation (3.7) with respect to ϕ as follow.

$$K_\phi(\phi) = K_L \left(r^2 \cos \phi - \frac{\ell r^2 \cos \phi}{L_\phi(\phi)} + \frac{\ell r^4 \sin^2 \phi}{L_\phi^3(\phi)} \right) \quad (3.8)$$

The change of K_ϕ is shown in figure 5-(a). The horizontal axis shows ϕ (0~180 [degree]). Link L is assumed to be an 8[mm]×16[mm] square pole (material : A2017 aluminum alloy) with length 30[mm] and $r = 16$ [mm], $K_L = 1.1 \times 10^8$ [N/m] are set. Though K_ϕ becomes a negative value when ϕ is more than 113[degree], the direction of the restorative force does not change because the accumulated energy E increases monotonically as shown in figure 5-(b).

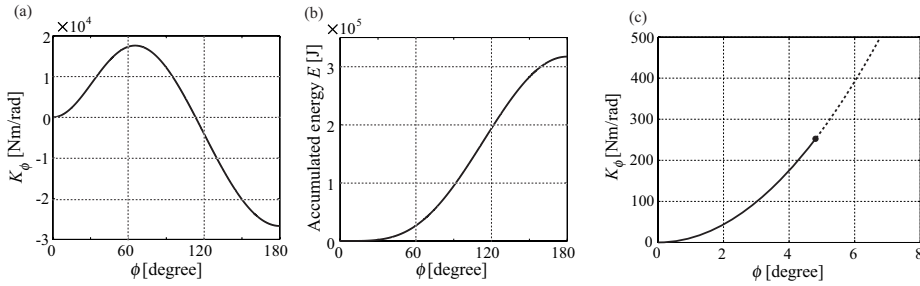


Figure 5. Stiffness and accumulated energy

Actually, the length of link L dose not change so much, and the area of $\phi = 0 \sim 8$ [degree] is zoom displayed in figure 5-(c). The point with circle means Yield Point of link L (with 0.1% strain). In this point, ϕ is 4.81[degree] and K_ϕ is 256[Nm/rad], which is equivalent to the torsional stiffness of duralumin cylinder with 7.5[mm] diameter and 30[mm] length. From this figure, it is clear that the stiffness of this mechanism has large change according to ϕ and zero stiffness is realized at $\phi = 0$.

3.4 Experimental evaluation of nonlinear stiffness

The stiffness of the designed mechanism is measured by experiments. A torque-load by a weight(0.010~4.0[kg]) is added to this mechanism and the rotation angle ϕ is measured. We design two types of the link L as shown in figure 6. One is a normal link without slits, another is a spring link with slits. The results are shown in figure 7-(a). The relationship between torque τ and rotation angle ϕ has high nonlinearity. Stiffness of the mechanism with each link is calculated. The results are shown in figure 7-(b). The theoretical values are shown together. The spring constant of each link is obtained from Finite Element Method (FEM). In both results, the experimental results show lower stiffness than the theoretical values, which is because the strains are caused also in the parts other than link L and backlash of the bearing is not small. These results show the zero-stiffness at $\phi = 0$ and high nonlinearity of the stiffness according to the change of ϕ .

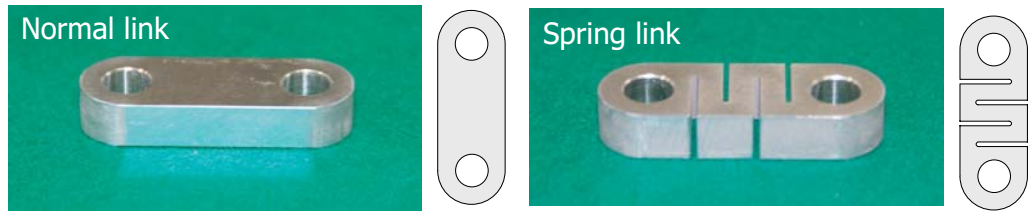


Figure 6. Two types of designed link L

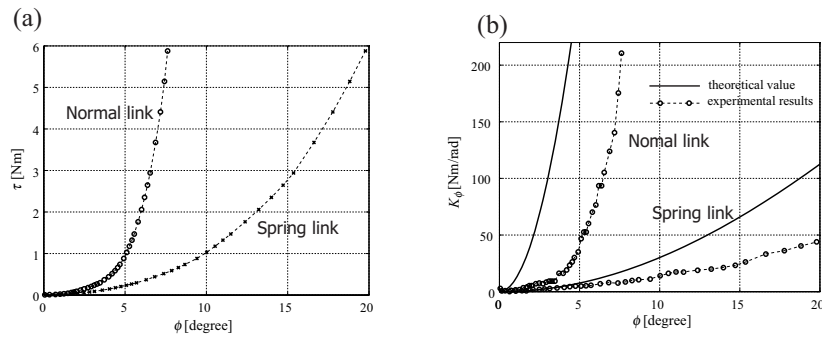


Figure 7. Torque τ and stiffness K_ϕ with respect to rotation angle ϕ

4 Evaluation of the effectiveness of high nonlinear stiffness

4.1 Four-legged robot

A four-legged robot with the proposed mechanism on the knee joint is designed. Four-legged robot requires (a) High softness to absorb the impact force on landing and (b) High stiffness to support the body weight and to yield high power for motion.



Figure 8. Four-legged robot

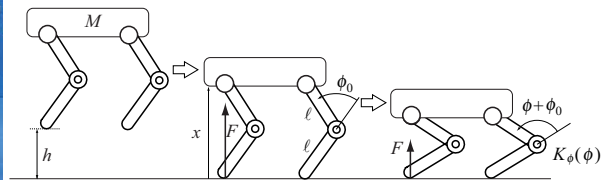


Figure 9. Robot motion on landing

Each leg has three degrees of freedom. Two DOF on the base (z -axis and x -axis) and one on the knee (x -axis). 60[W] DC motor and 1:50 reduction gear are used for each joint. The

size of this robot is about 350[mm](width) \times 450[mm](length) \times 450[mm](height) and the weight is about 15[kg]. Figure 8 shows the photograph of the designed robot and knee joint with the proposed mechanism. The proposed mechanism is indicated by circle.

4.2 Simulation for evaluation of the effectiveness of nonlinear stiffness

To evaluate the effectiveness of nonlinearity of the stiffness, we calculate the grounding force in landing. As shown in figure 9, the robot falls from the height h and lands. Because of the body weight M , the knee joints bends ϕ which yields the torque by the stiffness to support the body. The reaction forces from the ground on landing are shown in figure 10-(a). We set $h = 1$ [m],

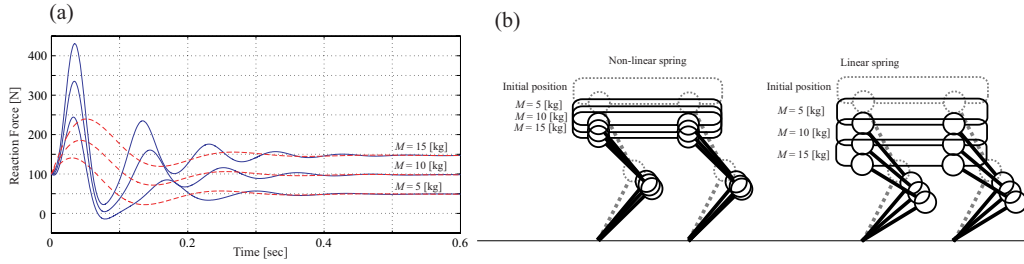


Figure 10. Reaction force on landing and robot motion

the length of the legs $\ell = 0.2$ [m] and $M = 5, 10, 15$ [kg]. The solid lines shows the results with the proposed mechanism (nonlinear spring) on the knee joint. For comparison, the dashed line shows when a linear torsional spring is used. The spring constant of the linear spring is set so that the final value of x with linear spring is equal to that of with nonlinear spring when $M = 5$. The damping parameter of the knee joint is selected appropriately. Figure 10-(b) shows the final positions of the robot. These results show that when the linear spring is used, the softness is obtained because the rigid joints causes infinite number of F .

Figure 11 shows the walk motion of the robot with the rigid joint, with the linear spring and with the nonlinear spring. These figures show as follows.

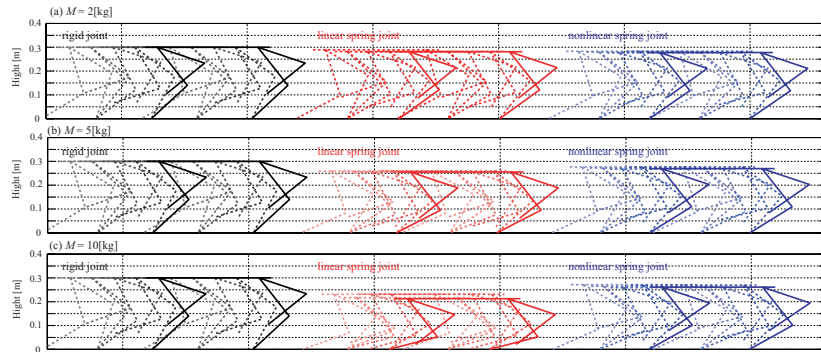


Figure 11. Walk motion of the robot

1. When we use the linear spring, the body height through the motion becomes lower according to the larger mass.

2. When we use the nonlinear spring, the change of the body height is small in spite of the increase of the body weight.

And we can conclude that the proposed mechanism realizes the high stiffness to support the body weight and to transmit high power for motion.

5 Conclusions

In this paper, we develop a torque transmission mechanism with nonlinear passive stiffness. The results of this paper are as follows.

- Based on mechanical singularity of the closed kinematic chain, zero-stiffness is realized.
- Zero-stiffness and nonlinear stiffness of the proposed mechanism are analyzed based on the kinematic constraints and they are evaluated by the experiments.
- A four-legged robot is designed with the proposed mechanism on knee joint.
- The effectiveness of high nonlinear stiffness of the proposed mechanism is shown by the landing and walking simulations.

Acknowledgment

This research is supported by the “Motion emergence and mutual progression of robot body and intelligence from the dynamical point of view” under Grants-in-Aid for Scientific Research (Category Encouragement of Young Scientists (A)) of Japan Society for the Promotion of Science.

Bibliography

- H. Hanafusa and H. Asada. Stable prehension by a robot hand with elastic fingers. In *Proc. of the 7th International Symposium on Industrial Robots*, 1978.
- N. Hogan. Aimpedance control: An approach to manipulation: Part 1~3.
- N. Hogan. Mechanical impedance control in assistive devices and manipulators. In *Proc. of the 1980 Joint Automatic Control Conference*, 1980.
- K. F. L-Kovitz, J. E. Colgate, and S. D. R. Carnes. Design of components for programmable passive impedance. In *Proc. of IEEE International Conference on Robotics and Automation*, 1991.
- T. Morita, N. Tomita, T. Ueda, and S. Sugano. Development of force-controlled robot arm using mechanical impedance adjuster. In *Proc. of IEEE International Conference on Intelligent Robots and Systems*, 1999.
- M. Okada, Y. Nakamura, and S. Ban. Design of programmable passive compliance shoulder mechanism. In *Proc. of IEEE International Conference on Robotics and Automation*, 2001.
- R. P. C. Paul and B. Shimano. Compliance and control. In *Proc. of the 1976 Joint Automatic Control Conference*, 1976.
- J. K. Salisbury. Active stiffness control of a manipulator in cartesian coordinates. In *Proc. of the IEEE Conference on Decision and Control*, 1980.
- J. Yamaguchi, D. Nishino, and A. Takanishi. Realization of dynamic biped walking varying joint stiffness using antagonistic driven joints. In *Proc. of the 1998 IEEE International Conference on Robotics and Automation*, 1998.